

Diffusion of cosmic rays in MHD turbulence with magnetic mirrors

ALEX LAZARIAN^{1,2} AND SIYAO XU³

¹*Department of Astronomy, University of Wisconsin, 475 North Charter Street, Madison, WI 53706, USA*

²*Center for Computation Astrophysics, Flatiron Institute, 162 5th Ave, New York, NY 10010*

³*Institute for Advanced Study, 1 Einstein Drive, Princeton, NJ 08540, USA^a*

ABSTRACT

As the fundamental physical process with many astrophysical implications, the diffusion of cosmic rays (CRs) is determined by their interaction with magnetohydrodynamic (MHD) turbulence. We consider the magnetic mirroring effect arising from MHD turbulence on the diffusion of CRs. Due to the intrinsic superdiffusion of turbulent magnetic fields, CRs with large pitch angles that undergo mirror reflection, i.e., bouncing CRs, are not trapped between magnetic mirrors, but move diffusively along the magnetic field, leading to a new type of parallel diffusion. This diffusion is in general slower than the diffusion of non-bouncing CRs with small pitch angles that undergo gyroresonant scattering. The critical pitch angle at the balance between magnetic mirroring and pitch-angle scattering is important for determining the diffusion coefficients of both bouncing and non-bouncing CRs and their scalings with the CR energy. We find non-universal energy scalings of diffusion coefficients, depending on the properties of MHD turbulence.

1. INTRODUCTION

Charged energetic particles or cosmic rays (CRs) are an important ingredient in the physical processes in space and astrophysical environments. It is customary to use the term “energetic particles” in space physics. The theoretical understanding on their acceleration and diffusion in the Solar atmosphere, solar wind, Earth magnetosphere, and heliosphere is important for studying the properties of the interplanetary magnetic field, solar modulation of Galactic CRs, and space weather forecasting (Parker 1965; Jokipii 1971; Singer et al. 2001).

The energetic particles with higher energies outside our direct neighborhood, i.e., of Galactic and extragalactic origin, are usually referred to as CRs. The knowledge on the acceleration and diffusion of CRs is essential for probing their sources, explaining their chemical composition, studying their roles in ionizing molecular gas and circumstellar discs (e.g., Schlickeiser et al. 2016; Padovani et al. 2018), driving galactic winds (e.g., Ipavich 1975; Holguin et al. 2019), and feedback heating in clusters of galaxies (e.g., Guo & Oh 2008; Brunetti & Jones 2014), as well as modeling the synchrotron foreground emission for cosmic microwave background (CMB) radiation and redshifted 21 cm radiation (e.g., Cho & Lazarian 2002a; Cho et al. 2012). In this work, we focus on the diffusion physics that is generally applicable to energetic particles of Solar origin and CRs. Thus we do not distinguish between them and will only use the term “CRs”.

The diffusion of CRs is governed by their interaction with turbulent magnetic fields. This has been a subject of intensive research (Jokipii 1966; Kulsrud & Pearce 1969; Schlickeiser & Miller 1998; Giacalone & Jokipii 1999). The development of modern theories of magnetohydrodynamic (MHD) turbulence over the past few decades (Goldreich & Sridhar 1995; Lazarian & Vishniac 1999; Cho & Vishniac 2000; Maron & Goldreich 2001; Lithwick & Goldreich 2001; Cho et al. 2002; Cho & Lazarian 2003; Beresnyak 2014; Kowal et al. 2017, see also the book by Beresnyak & Lazarian 2019) leads to a paradigm shift to the standard diffusion models of CRs, whose predictions have been challenged by recent multifrequency observations and direct CR measurements (Nava & Gabici 2013; Orlando 2018; Gabici et al. 2019; Amato & Casanova 2021).

Based on the modern MHD turbulence theories that have been tested with both simulations (Cho & Vishniac 2000; Maron & Goldreich 2001; Cho & Lazarian 2003; Beresnyak 2014; Kowal & Lazarian 2010) and solar wind observations (Horbury et al. 2008; Luo & Wu 2010; Forman et al. 2011), new findings on the pitch-angle scattering, stochastic acceleration, spatial diffusion of CRs along the magnetic field (Chandran 2000a; Yan & Lazarian 2002, 2004; Brunetti & Lazarian 2007; Yan & Lazarian 2008; Lynn et al. 2012; Xu & Yan 2013; Xu & Lazarian 2018; Sioulas et al. 2020; Lemoine & Malkov 2020), superdiffusion and diffusion perpendicular to the mean magnetic field (Yan & Lazarian 2008; Lazarian & Yan 2014), propagation of CRs in weakly ionized astrophysical media (Xu et al. 2016), and interactions of CRs with relativistic MHD turbulence (Demidem et al. 2020) have been reported. These studies bring significant changes to the traditional picture of CR propagation using ad hoc models of MHD turbulence (e.g., Matthaeus et al. 1990; Kóta & Jokipii 2000; Qin et al. 2002) and shed light on some long-standing

lazarian@astro.wisc.edu; sxu@ias.edu

^a Hubble Fellow

problems and observational puzzles (e.g., Palmer 1982; Evoli & Yan 2014; López-Barquero et al. 2016; Krumholz et al. 2020).

In addition to the pitch-angle scattering, it was found that the propagation of CRs can also be affected by magnetic mirror reflection when CRs interact with large-scale magnetic irregularities (Fermi 1949; Noerdlinger 1968; Cesarsky & Kulsrud 1973; Klepach & Ptuskin 1995; Chandran 2000b), which provides a solution to the 90° problem of the quasi-linear theory (QLT, Jokipii 1966) for pitch-angle scattering. In these earlier studies, the magnetic mirroring effect is invoked for trapping CRs that bounce back and forth between two mirror points, and it has not been considered within the framework of modern theories of MHD turbulence. In MHD turbulence, compressions of magnetic fields, which are generated by pseudo-Alfvén modes in an incompressible medium and slow and fast modes in a compressible medium, naturally give rise to the mirroring effect over a range of length scales following the energy cascade of turbulence. The interaction of CRs with magnetic mirrors is regulated by the dynamics of turbulent magnetic fields. Therefore, the intrinsic perpendicular superdiffusion of turbulent magnetic fields (Lazarian & Vishniac 1999; Eyink et al. 2013; Lazarian & Yan 2014) and its interaction with the parallel diffusion should be taken into account when studying the CR diffusion under the mirroring effect.

By using the numerically tested scalings of MHD turbulence (Cho & Lazarian 2003), Xu & Lazarian (2020) (hereafter XL20) investigated the scattering of CRs with the mirroring effect considered. There we confirmed the dominant role of fast modes in gyroresonant scattering (Yan & Lazarian 2002), and we found that the resulting diffusion coefficient is significantly smaller than that in the absence of magnetic mirroring. In this work, toward a more complete picture of the parallel diffusion of CRs, we will focus on the CRs that bounce among multiple magnetic mirrors, i.e., bouncing CRs, in MHD turbulence and the effect of magnetic mirroring on their diffusion. In Section 2, we introduce the perpendicular superdiffusion of both turbulent magnetic fields and CRs and its effect on the parallel diffusion of bouncing CRs. In Sections 3 and 4, we formulate the diffusion coefficients of bouncing CRs in compressible and incompressible MHD turbulence, respectively. In Section 5, we consider the exchange between bouncing and non-bouncing CRs and discuss the averaged diffusion coefficient. Finally, the discussion and the summary of our main results are given in Sections 6 and 7.

2. SPATIAL DIFFUSION OF BOUNCING PARTICLES

2.1. Magnetic mirrors in MHD turbulence

MHD turbulence can be decomposed into Alfvén, slow, and fast modes (Lithwick & Goldreich 2001; Cho & Lazarian 2003). Alfvén modes induce magnetic field wandering, which accounts for the superdiffusion of CRs perpendicular to the mean magnetic field. Slow modes are passively mixed by Alfvén modes and have the same anisotropic scaling as Alfvén modes. Fast modes have an independent energy cascade and isotropic energy distribution. Compressive

slow and fast modes act as magnetic mirrors that result in bouncing of particle among the mirror points. Their detailed statistical properties are presented in Appendix.

The magnetic mirroring effect caused by static magnetic bottles is well known in plasma physics (e.g., Post 1958; Budker 1959; Noerdlinger 1968; Kulsrud & Pearce 1969). A particle with the Larmor radius smaller than the variation scale of the magnetic field preserves its adiabatic invariant, i.e. $p_\perp^2/B = \text{const}$. It implies

$$\frac{p_\perp^2}{B_0} = \frac{p^2}{B_0 + \delta b} \quad (1)$$

for the condition of magnetic mirroring, where B_0 and $B_0 + \delta b$ are the magnetic field strengths in the weak and strong magnetic field regions, and p is the total momentum of the particle. The particles with $\mu < \mu_{lc}$, where μ is the pitch-angle cosine and μ_c satisfies

$$\mu_{lc}^2 = \cos^2 \theta_{lc} = \frac{\delta b}{B_0 + \delta b}, \quad (2)$$

are subject to magnetic mirroring. Here θ_{lc} is angular size of the loss cone for escaping particles with smaller pitch angles. For slow and fast modes in MHD turbulence with a spectrum of magnetic fluctuations, there is $\delta b = b_k$. When b_k at wavenumber k is significantly smaller than the mean magnetic field strength B_0 , the above expression can be approximated by

$$\mu_{lc}^2 \approx \frac{b_k}{B_0}. \quad (3)$$

The amplitude of b_k depends on the driven magnetic perturbations δB_s and δB_f of slow and fast modes. Their relation depends on the compressibility of the medium. In a pressure dominated medium with the sonic Mach number $M_s = V_L/c_s < 1$ and $\beta = P_{\text{gas}}/P_{\text{mag}} > 1$, where V_L is the driven turbulent velocity, c_s is the sound speed, and P_{gas} and P_{mag} are gas/plasma and magnetic pressures, δB_s is expected to be larger than δB_f . In the opposite limit of magnetically dominated medium with $\beta < 1$, there is $\delta B_s < \delta B_f$.

In the literature, particles with $\mu < \mu_{lc}$ are considered “trapped” in magnetic bottles and thus they cannot diffuse. However, as we will show below (Section 2.3), this is an erroneous notion. In fact, for 3D propagation in MHD turbulence, magnetic mirroring results in a new type of parallel diffusion of bouncing particles.

2.2. Perpendicular superdiffusion

CRs following magnetic field lines ¹ undergo pitch-angle scattering via the interaction with small-scale magnetic fluctuations and bouncing among magnetic mirrors (see above). In the meantime, the dispersion of their trajectories in the

¹ In the presence of turbulence, CRs follow the magnetic flux tubes averaged within their gyro-orbit. We nevertheless adopt the generally accepted way to describe magnetic fields as “magnetic field lines”.

direction perpendicular to the mean magnetic field is determined by the dispersion of magnetic field lines. This dispersion increases with the propagation distance of CRs along the magnetic field and accounts for the perpendicular diffusion of CRs, as pointed out by Jokipii (1966). The superdiffusive nature of this dispersion was later found by Lazarian & Vishniac (1999) when they analytically quantified the magnetic field wandering induced by the Alfvénic component² of MHD turbulence for both super-Alfvénic ($M_A = V_L/V_A > 1$) and sub-Alfvénic ($M_A < 1$) turbulence, where V_A is the Alfvén speed. We note that the perpendicular superdiffusion is with respect to the mean magnetic field in sub- and trans-Alfvénic ($M_A = 1$) turbulence, and with respect to the local mean field, i.e., the magnetic field averaged over scales less than $l_A = LM_A^{-3}$ in super-Alfvénic turbulence (Lazarian 2006), where L is the turbulence driving scale, and l_A is the scale where the local turbulent velocity becomes equal to V_A . For the turbulent motions on scales larger than l_A , the effect of magnetic field is subdominant, and they gradually get isotropic, similar to the hydrodynamic Kolmogorov turbulence.

For sub-Alfvénic turbulence, there exists a scale $l_{\text{tran}} = LM_A^2$ for the transition from the weak turbulence over the scales $[l_{\text{tran}}, L]$ to the strong turbulence on smaller length scales. In the weak turbulence regime, the magnetic fields exhibit normal diffusion, i.e. the mean squared separation between magnetic field lines increases with $l_{\text{tran}}s$, where s is the distance measured along the magnetic field lines (Lazarian & Vishniac 1999).

We next consider the divergence of magnetic field lines over scales less than l_{tran} . Naturally, when one follows the magnetic field line over the parallel scale l_{\parallel} of a turbulent eddy, the magnetic field line has its perpendicular displacement equal to the transverse size l_{\perp} of the eddy. As l_{\perp} can be both positive and negative, the dispersion $\langle y^2 \rangle$ of magnetic field lines increases as

$$d\langle y^2 \rangle \approx l_{\perp}^2 \frac{ds}{l_{\parallel}}, \quad (4)$$

where ds is the distance measured along the magnetic field line, and the bracket denotes an ensemble average. Using the above relation and the scaling relation between l_{\parallel} and l_{\perp} for sub-Alfvénic turbulence (Lazarian & Vishniac (1999), see also Appendix A), one can find

$$d\langle y^2 \rangle \approx \langle y^2 \rangle^{2/3} M_A^{4/3} L^{-1/3} ds. \quad (5)$$

If the expression on the right-hand side were “constant $\times ds$ ”, Eq. (5) would describe the random walk of field lines. However, it has a power-law dependence on the field line separation with a positive power index, i.e. $\propto \langle y^2 \rangle^{2/3}$, leading to

² The separation of MHD turbulence into Alfvénic, slow and fast modes was demonstrated numerically in Cho & Lazarian (2002, 2003). The dominance of Alfvénic modes in terms of inducing magnetic field wandering was shown analytically in Lazarian & Vishniac (1999).

an accelerating superdiffusion as magnetic field lines spread out. The numerical demonstration of the superdiffusion of turbulent magnetic fields can be found in, e.g., Lazarian et al. (2004); Beresnyak (2013).

The physical explanation of the effect is the following. As we follow the magnetic field line the distance $\sim s$, the divergence rate of field lines increases with larger and larger turbulent eddies contributing to the dispersion of field line separations. A similar effect in hydrodynamic turbulence is related to the accelerated separation of a pair of test particles with time, which is known as Richardson dispersion (Richardson 1926). The accelerated divergence of magnetic field lines results in the superdiffusive behavior of field line separations. The analogy between the Richardson dispersion and the superdiffusion of magnetic fields introduced in Lazarian & Vishniac (1999) was discussed in detail in Eyink et al. (2011).

Eq. (5) also applies to the dispersion of separations of CRs that follow magnetic field lines. The resulting superdiffusive perpendicular divergence of CR trajectories was introduced and studied in Yan & Lazarian (2008); Lazarian & Yan (2014) and numerically tested by Xu & Yan (2013). The corresponding dispersion of separations of particles in the perpendicular direction is

$$\langle y^2 \rangle \sim l_{\perp}^2 \approx \frac{s^3}{L} M_A^4, \quad M_A < 1, \quad s < L. \quad (6)$$

Here s is the distance of particles measured along the magnetic field line. y can be identified with the displacement of particles perpendicular to the mean magnetic field.

The above expression can also be applied to super-Alfvénic turbulence at scales less than l_A , i.e., $s < l_A$. A detailed discussion on the perpendicular diffusion of CRs in different turbulence regimes is provided in Lazarian & Yan (2014).

2.3. Parallel bouncing diffusion

The effect of magnetic mirrors on trapping particles was extensively studied in the literature (e.g., Noerdlinger 1968; Kulsrud & Pearce 1969; Cesarsky & Kulsrud 1973). There it was assumed that the trapped particles undergo oscillatory motions between two mirror points of a magnetic bottle, without cumulative diffusion along the magnetic field. As the main difference between this work and earlier studies, here we consider the existence of Alfvénic component of turbulence and the resulting perpendicular superdiffusion of magnetic fields and CRs. In the presence of Alfvénic turbulence, the superdiffusion of magnetic fields does not allow the particles to be trapped in the same magnetic bottle.

For every crossing of a magnetic bottle induced by the compressive component of MHD turbulence with a size s , the particle experiences perpendicular superdiffusion with the perpendicular displacement y given by Eq. (6). As a result, the particle escapes the magnetic bottle within one crossing time and then encounters another magnetic bottle with a perpendicular distance y from the previous magnetic bottle. The bouncing among the mirror points of different

magnetic bottles leads to the diffusive motion of particles along the magnetic field. We term this parallel diffusion arising from bouncing as “parallel bouncing diffusion” to distinguish it from the traditional CR parallel diffusion associated with the resonance scattering (see [Schlickeiser 2002](#)). We illustrate the parallel bouncing diffusion in Fig. 1. CRs that follow diffusing magnetic field lines are not trapped, but move diffusively parallel to the magnetic field when bouncing among different magnetic mirrors.

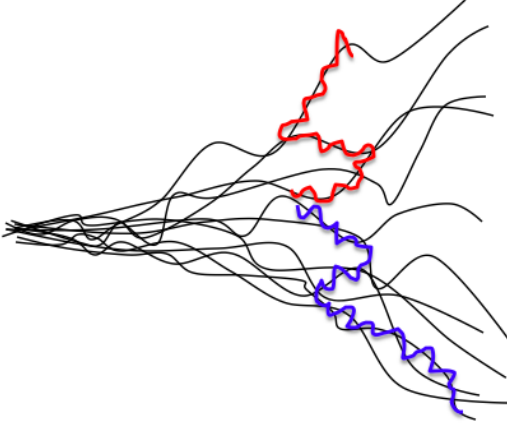


Figure 1. Because of the perpendicular superdiffusion of particles following diffusing magnetic field lines, particles that undergo bouncing move diffusively along the magnetic field. Thin lines represent magnetic field lines. Thick lines represent the trajectories of two particles whose initial separation is small.

3. PARALLEL DIFFUSION OF BOUNCING PARTICLES INDUCED BY FAST MODES IN COMPRESSIBLE MHD TURBULENCE

3.1. Bouncing and non-bouncing particles

In compressible MHD turbulence, if fast modes carry a significant fraction of the injected turbulent energy, they act as the main agent for scattering particles ([Yan & Lazarian 2002, 2004](#)). More recently, XL20 identified the important role of fast modes in both bouncing and scattering CRs. XL20 studied the parallel diffusion associated with the gyroresonant scattering of non-bouncing particles. Here we will also analyze the parallel diffusion of bouncing particles. The effects of transit-time damping (TTD) acceleration on scattering and bouncing will be discussed in our future work.

The scattering causes diffusion in pitch angle. In the quasilinear approximation ([Jokipii 1966](#)), for the gyroresonant scattering by fast modes, the pitch-angle diffusion coefficient is ([Voelk 1975](#))

$$D_{\mu\mu, \text{QLT}, f} = C_{\mu} \int d^3k \frac{k_{\parallel}^2}{k^2} [J_1'(x)]^2 I_f(k) R(k). \quad (7)$$

Here

$$C_{\mu} = (1 - \mu^2) \frac{\Omega^2}{B_0^2}, \quad x = \frac{k_{\perp} v_{\perp}}{\Omega} = \frac{k_{\perp}}{r_g^{-1}}, \quad (8)$$

B_0 is the mean magnetic field strength, v_{\perp} is the perpendicular component of particle velocity v , Ω is the gyrofrequency, r_g is the particle gyroradius, and k_{\parallel} and k_{\perp} are parallel and perpendicular components of wavenumber k . Besides,

$$I_f(k) = C_f k^{-\frac{7}{2}} \quad (9)$$

is the energy spectrum of fast modes ([Cho & Lazarian 2002b](#)), with

$$C_f = \frac{1}{16\pi} \delta B_f^2 L^{-\frac{1}{2}}, \quad (10)$$

where δB_f is the magnetic perturbation of fast modes at L , and

$$R = \pi \delta(\omega_k - v_{\parallel} k_{\parallel} + \Omega) \quad (11)$$

is the resonance function for gyroresonance in the quasilinear approximation, where ω_k is the wave frequency. We see that when the pitch angle approaches 90° , the above resonance condition cannot be satisfied with a limited range of k and decreasing magnetic fluctuation amplitude with increasing k , leading to the 90° problem³. For our analytical estimate, we can use the approximate expression of $D_{\mu\mu, \text{QLT}, f}$ ([Xu et al. 2016; Xu & Lazarian 2018](#))

$$D_{\mu\mu, \text{QLT}, f} \approx \frac{\pi}{56} \frac{\delta B_f^2}{B_0^2} \left(\frac{v}{L\Omega} \right)^{\frac{1}{2}} \Omega (1 - \mu^2) \mu^{\frac{1}{2}}. \quad (12)$$

We define the rate of change in μ due to scattering as the scattering rate (XL20),

$$\Gamma_{s, f} = \frac{2D_{\mu\mu, \text{QLT}, f}}{\mu^2} \approx \frac{\pi}{28} \frac{\delta B_f^2}{B_0^2} \left(\frac{v}{L\Omega} \right)^{\frac{1}{2}} \Omega (1 - \mu^2) \mu^{-\frac{3}{2}}. \quad (13)$$

In the presence of the stochastic magnetic mirrors induced by fast modes, the particles that satisfy the bouncing condition (see below) undergo the bouncing motions among different magnetic mirrors as discussed in Section 2.3. For particles with (see Eq. (3))

$$\mu \approx \sqrt{\frac{b_{fk}}{B_0}}, \quad (14)$$

the bouncing is dominated by the magnetic mirrors at k with the magnetic perturbation b_{fk} ([Cesarsky & Kulsrud 1973](#)), where

$$b_{fk} = \delta B_f (kL)^{-\frac{1}{4}} \quad (15)$$

according to the scaling of isotropic fast modes ([Cho & Lazarian 2002b](#)). The rate of the adiabatic change in μ due to the spatial variation of magnetic field is ([Cesarsky & Kulsrud 1973, XL20](#))

$$\begin{aligned} \Gamma_{b, f} &= \left| \frac{1}{\mu} \frac{d\mu}{dt} \right| = \frac{v}{2B_0} \frac{1 - \mu^2}{\mu} b_{fk} k \\ &= \frac{v}{2L} \frac{\delta B_f^4}{B_0^4} \frac{1 - \mu^2}{\mu^7} \end{aligned} \quad (16)$$

³ The vanishing scattering close to 90° and infinite mean free path in the quasi-linear theory is known as the 90° problem ([Fisk et al. 1974](#)).

at $\mu > \mu_{\min,f}$, where

$$\mu_{\min,f} = \sqrt{\frac{b_{fk}(r_g)}{B_0}} = \sqrt{\frac{\delta B_f}{B_0}} \left(\frac{r_g}{L}\right)^{\frac{1}{8}}, \quad (17)$$

and $b_{fk}(r_g)$ is the magnetic perturbation at r_g . At $\mu < \mu_{\min,f}$, the bouncing rate is

$$\begin{aligned} \Gamma_{b,f} &= \frac{v}{2B_0} \frac{1-\mu^2}{\mu} b_{fk}(r_g) r_g^{-1} \\ &= \frac{v}{2r_g} \frac{\delta B_f}{B_0} \left(\frac{r_g}{L}\right)^{\frac{1}{4}} \frac{1-\mu^2}{\mu}. \end{aligned} \quad (18)$$

At the balance between scattering and bouncing, i.e., $\Gamma_{s,f} = \Gamma_{b,f}$, one can find the cutoff μ (Eqs. (13) and (16)),

$$\mu_c \approx \left[\frac{14}{\pi} \frac{\delta B_f^2}{B_0^2} \left(\frac{v}{L\Omega}\right)^{\frac{1}{2}} \right]^{\frac{2}{11}}, \quad (19)$$

in agreement with the result in XL20. We define the particles with $\mu < \mu_c$ as ‘‘bouncing particles’’ and those with $\mu > \mu_c$ as ‘‘non-bouncing’’ particles. Their motions are dominated by bouncing and scattering, respectively. As shown in Fig. 2, μ_c increases with the CR energy E_{CR} until reaching its maximum value

$$\mu_{c,\max} = \sqrt{\frac{\delta B_f}{B_0 + \delta B_f}}. \quad (20)$$

Here as an illustration, we consider CR protons, the magnetic field strength $\delta B_f = B_0 = 3\mu\text{G}$, and $L = 30$ pc as the driving scale of interstellar turbulence.

3.2. Parallel diffusion of bouncing particles

When the bouncing condition $\mu < \mu_c$ is satisfied, the parallel diffusion of particles with μ is regulated by the bouncing effect. Based on the relations in Eqs (14) and (15), bouncing particles diffuse along the magnetic field with a step size

$$k^{-1} = L \left(\frac{\delta B_f}{B_0}\right)^{-4} \mu^8 \quad (21)$$

for $k^{-1} > r_g$, or equivalently $\mu > \mu_{\min,f}$. At $\mu < \mu_{\min,f}$, the step size of parallel diffusion is r_g , corresponding to the Bohm diffusion. The maximal step size of bouncing particles corresponds to μ_c ,

$$k_c^{-1} = L \left(\frac{\delta B_f}{B_0}\right)^{-4} \mu_c^8. \quad (22)$$

It decreases with the increase of $\delta B_f/B_0$ (see Eq. (19)) and should not exceed L . The bouncing of the particles with $\mu > \mu_c$ by the magnetic fluctuations on scales larger than k_c^{-1} is less efficient than their gyroresonant scattering by small-scale magnetic fluctuations.

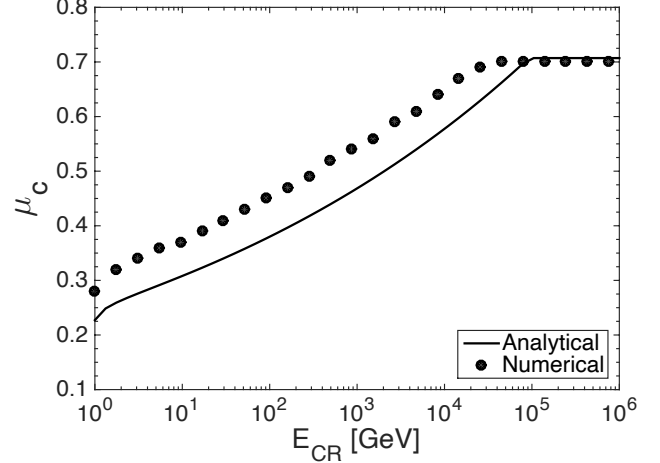


Figure 2. μ_c as a function of E_{CR} for fast modes. The analytical approximation is given by Eq. (19). The numerical result is obtained based on the numerical evaluation of Eq. (7).

The corresponding parallel diffusion coefficient arising from bouncing is

$$D_{\parallel,f,b}(\mu) = \begin{cases} v\mu k^{-1} = vL \left(\frac{\delta B_f}{B_0}\right)^{-4} \mu^9, & \mu_{\min,f} < \mu < \mu_c, \\ v\mu r_g, & \mu < \mu_{\min,f}. \end{cases} \quad (23a) \quad (23b)$$

The strong dependence on μ comes from the μ -dependence of the size of the dominant magnetic mirror field (Eq. (21)). The bouncing makes the parallel diffusion of CRs with a smaller μ more inefficient. This is opposite to the expectation from the quasi-linear scattering theory.

We first assume an isotropic pitch angle distribution for a simple analytical estimate of the parallel diffusion coefficient. By integrating $D_{\parallel,f,b}(\mu)$ over μ , we find the parallel diffusion coefficient as a sum of the contributions from the multi-scale magnetic mirror field for bouncing particles with different μ ,

$$\begin{aligned} D_{\parallel,f,b} &= \int_0^{\mu_c} D_{\parallel,f,b}(\mu) d\mu \\ &\approx \frac{1}{10} vL \left(\frac{\delta B_f}{B_0}\right)^{-4} \mu_c^{10}, \end{aligned} \quad (24)$$

where we consider that the contribution from $D_{\parallel,f,b}(\mu)$ at $\mu < \mu_{\min,f}$ is small.

In the situation with an anisotropic pitch angle distribution resulting from the anisotropic scattering (see Eq. (12)), we focus on the pitch-angle diffusion and use the spatially averaged Fokker-Planck equation

$$\frac{\partial f}{\partial t} = \frac{\partial}{\partial \mu} \left[D_{\mu\mu} \frac{\partial f}{\partial \mu} \right] \quad (25)$$

to derive the particle distribution function f under the effect of scattering. If the steady state, i.e., $\partial f/\partial t = 0$, can be reached, we have

$$D_{\mu\mu} \frac{df}{d\mu} = C, \quad (26)$$

where $-C$ is the constant flux of particles in μ space. The steady-state solution is

$$f(\mu) = -C \int_{\mu}^{\mu_c} \frac{d\mu'}{D_{\mu\mu}(\mu')} + f(\mu_c). \quad (27)$$

To simplify the evaluation of $f(\mu)$, we further adopt the boundary condition

$$f(\mu_c) = 0 \quad (28)$$

by assuming that scattering is inefficient and the scattering particles at $\mu > \mu_c$ instantly escape from the system. This assumption is approximately valid when the diffusion coefficient of the non-bouncing particles is much larger than that of the bouncing particles. We then normalize f

$$f' = \frac{f}{\int_0^{\mu_c} f d\mu} \quad (29)$$

to have unit integral,

$$\int_0^{\mu_c} f' d\mu = 1. \quad (30)$$

The parallel diffusion coefficient of bouncing particles under the consideration of anisotropic pitch angle distribution is then

$$D_{\parallel,f,b} = \int_0^{\mu_c} D_{\parallel,f,b}(\mu) f' d\mu, \quad (31)$$

where $D_{\parallel,f,b}(\mu)$ is given by Eq. (23). It is evident that the above calculation of $D_{\parallel,f,b}$ for bouncing particles depends on $D_{\mu\mu}$ that originates from scattering.

To provide an example for illustrating the parallel diffusion of bouncing particles, in Fig. 3, we present the numerically calculated $D_{\parallel,f,b}$ as a function of E_{CR} and its analytical approximation (Eq. (24)). The same parameters as used in Fig. 2 are adopted. We see that the simplification by using an isotropic pitch angle distribution in Eq. (24) does not significantly affect the result. This is because $D_{\mu\mu,\text{QLT},f}$ and the

resulting $f(\mu)$ are not significantly anisotropic.⁴ The analytical estimate has the energy dependence as $D_{\parallel,f,b} \propto E_{\text{CR}}^{10/11}$ for relativistic particles (Eqs. (19) and (24)), which is close to $D_{\parallel,f,b} \propto E_{\text{CR}}$. The numerical result is a bit shallower and can be fitted by $D_{\parallel,f,b} \propto E_{\text{CR}}^{0.7}$. The discrepancy between the analytical and numerical results at the high-energy end comes from the energy dependence of $D_{\parallel,f,b}(\mu)$ at $\mu < \mu_{\min,f}$ (Eq. (23)), which is not taken into account in the analytical approximation.

As a comparison, in Fig. 3 we also add the parallel diffusion coefficient of non-bouncing particles determined by the gyroresonant scattering by fast modes derived in XL20. The analytical approximation is given by

$$\begin{aligned} D_{\parallel,f,nb} &= \frac{v^2}{4} \int_{\mu_c}^1 d\mu \frac{(1-\mu^2)^2}{D_{\mu\mu,\text{QLT},f}(\mu)} \\ &\approx \frac{28}{5\pi} \frac{B_0^2}{\delta B_f^2} \left(\frac{v}{L\Omega} \right)^{-\frac{1}{2}} \frac{v^2}{\Omega} [4 - \sqrt{\mu_c}(5 - \mu_c^2)], \end{aligned} \quad (32)$$

where the lower bound in integration is given by μ_c (see Cesarsky & Kulsrud 1973). The resulting $D_{\parallel,f,nb}$ for non-bouncing particles is shallower than $\propto E_{\text{CR}}^{0.5}$ except for the high-energy end with a constant μ_c . Its scaling with E_{CR} is not an exact power law, but can be approximated by $\propto E_{\text{CR}}^{1/3}$ (see Fig. 3). We see that there is $D_{\parallel,f,b} < D_{\parallel,f,nb}$ for all CR energies considered here. This justifies the boundary condition in Eq. (28). The bouncing particles have a more inefficient diffusion compared with the non-bouncing particles.

We note that in the above illustration, we assume $\delta B_f = B_0$. In this case with $\delta B_f < B_0$, both bouncing and non-bouncing particles would have larger diffusion coefficients.

4. PARALLEL DIFFUSION OF BOUNCING PARTICLES IN INCOMPRESSIBLE MHD TURBULENCE

4.1. Trans-Alfvénic turbulence

It is known that the gyroresonant scattering with both Alfvén modes and pseudo-Alfvén modes is inefficient especially for relatively low-energy CRs due to the scale-dependent anisotropy of MHD turbulence (Chandran 2000a; Yan & Lazarian 2002). Yan & Lazarian (2002) thus argued that fast modes in the interstellar medium mainly contribute to the scattering of Galactic GeV CRs. However, when fast modes are damped, plasma β is large, or the injected energy of fast modes is small, additional sources for confining CRs are needed. Next we study incompressible MHD turbulence or compressible MHD turbulence with a very small energy fraction in fast modes to address the bouncing effect induced by pseudo-Alfvén (slow) modes, which was found by XL20 to be important for affecting the parallel diffusion of CRs in incompressible MHD turbulence.

⁴ The result derived from isotropic pitch angle distribution is supposed to be larger than the one derived from anisotropic distribution. Our analytical approximation underestimates the former due to the underestimation of μ_c (see Fig. 2).

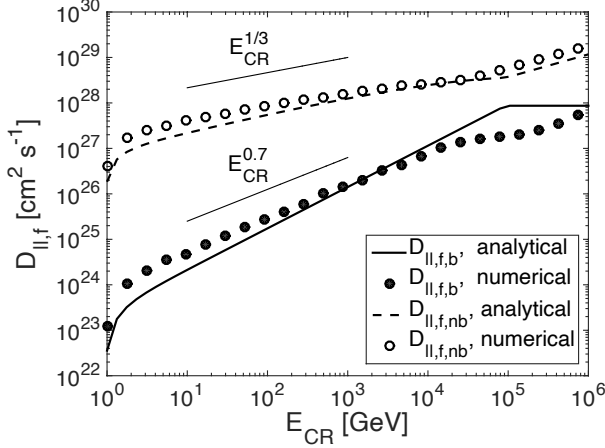


Figure 3. Parallel diffusion coefficients $D_{\parallel,f,b}$ of bouncing CRs and $D_{\parallel,f,nb}$ of non-bouncing CRs as a function of CR energy in compressible MHD turbulence with fast modes dominating both bouncing and scattering. The analytical approximations are given by Eq. (24) and Eq. (32), respectively.

The pitch-angle diffusion coefficients for gyroresonant interactions with Alfvén and pseudo-Alfvén modes in the quasi-linear approximation are (Voelk 1975),

$$D_{\mu\mu,QLT,A} = C_{\mu} \int d^3k x^{-2} [J_1(x)]^2 I_A(k) R(k), \quad (33)$$

and

$$D_{\mu\mu,QLT,s} = C_{\mu} \int d^3k \frac{k_{\parallel}^2}{k^2} [J_1'(x)]^2 I_s(k) R(k). \quad (34)$$

The magnetic energy spectra are (Cho et al. 2002)

$$I_A(k) = C_A k_{\perp}^{-\frac{10}{3}} \exp\left(-L^{\frac{1}{3}} \frac{k_{\parallel}}{k_{\perp}^{\frac{2}{3}}}\right), \quad C_A = \frac{1}{6\pi} \delta B_A^2 L^{-\frac{1}{3}} \quad (35)$$

for Alfvén modes, and

$$I_s(k) = C_s k_{\perp}^{-\frac{10}{3}} \exp\left(-L^{\frac{1}{3}} \frac{k_{\parallel}}{k_{\perp}^{\frac{2}{3}}}\right), \quad C_s = \frac{1}{6\pi} \delta B_s^2 L^{-\frac{1}{3}} \quad (36)$$

for pseudo-Alfvén modes, where δB_A and δB_s are their magnetic perturbations at L . The corresponding scattering

rate with contributions from both Alfvén and pseudo-Alfvén modes is

$$\Gamma_{s,inc} = \frac{2(D_{\mu\mu,QLT,A} + D_{\mu\mu,QLT,s})}{\mu^2}. \quad (37)$$

Besides scattering, pseudo-Alfvén modes also generate magnetic mirrors accounting for the bouncing of CRs. The particles with

$$\mu \approx \sqrt{\frac{b_{sk}}{B_0}} \quad (38)$$

mainly undergo the bouncing motion at k_{\parallel} , where the magnetic perturbation of pseudo-Alfvén modes is

$$b_{sk} = \delta B_s (k_{\perp} L)^{-\frac{1}{3}} = \delta B_s (k_{\parallel} L)^{-\frac{1}{2}} \quad (39)$$

based on the anisotropic scaling of MHD turbulence (Cho et al. 2002). The bouncing rate is (Cesarsky & Kulsrud 1973, XL20)

$$\begin{aligned} \Gamma_{b,s} &= \left| \frac{1}{\mu} \frac{d\mu}{dt} \right| = \frac{v}{2B_0} \frac{1-\mu^2}{\mu} b_{sk} k_{\parallel} \\ &= \frac{v}{2L} \aleph_s^2 \frac{1-\mu^2}{\mu^3} \end{aligned} \quad (40)$$

at $\mu > \mu_{min,s}$, where

$$\aleph_s = \frac{\delta B_s}{B_0}, \quad (41)$$

$$\mu_{min,s} = \sqrt{\frac{b_{sk}(r_g)}{B_0}} = \sqrt{\aleph_s} \left(\frac{r_g}{L}\right)^{\frac{1}{4}}, \quad (42)$$

and $b_{sk}(r_g)$ is the magnetic perturbation at $k_{\parallel} = 1/r_g$. At $\mu < \mu_{min,s}$, the bouncing rate becomes

$$\begin{aligned} \Gamma_{b,s} &= \frac{v}{2B_0} \frac{1-\mu^2}{\mu} b_{sk}(r_g) r_g^{-1} \\ &= \frac{v}{2r_g} \aleph_s \left(\frac{r_g}{L}\right)^{\frac{1}{2}} \frac{1-\mu^2}{\mu}. \end{aligned} \quad (43)$$

Here we note that as $\Gamma_{b,s}$ and $\Gamma_{b,f}$ (Eqs. (16) and (18)) have different μ dependence, in the presence of both slow and fast modes in compressible MHD turbulence, the relative importance between the bouncing effects induced by slow and fast modes can change with μ (see Section 5.2).

As found in XL20, because of the inefficient scattering by Alfvén and pseudo-Alfvén modes, the bouncing dominates over the gyroresonant scattering, i.e. $\Gamma_{b,s} > \Gamma_{s,inc}$, for $\mu < \mu_c$, and μ_c is given by its maximum value ⁵

$$\mu_c = \sqrt{\frac{\delta B_s}{B_0 + \delta B_s}}, \quad (44)$$

⁵ μ_c in incompressible MHD turbulence was approximated to be unity in XL20 for simplicity.

which is independent of E_{CR} .

The non-bouncing particles with $\mu > \mu_c$ are only poorly constrained by the inefficient scattering, and their diffusion coefficients are expected to be large (see Section 5). For the parallel diffusion of bouncing particles, the step size is

$$k_{\parallel}^{-1} = L\aleph_s^{-2}\mu^4 \quad (45)$$

at $\mu > \mu_{\text{min},s}$, or equivalently, $k_{\parallel}^{-1} > r_g$, and the step size is r_g at $\mu < \mu_{\text{min},s}$. Accordingly, the μ -dependent parallel diffusion coefficient is

$$D_{\parallel,\text{inc},b}(\mu) = \begin{cases} v\mu k_{\parallel}^{-1} = vL\aleph_s^{-2}\mu^5, & \mu_{\text{min},s} < \mu < \mu_c, \\ v\mu r_g, & \mu < \mu_{\text{min},s}. \end{cases} \quad (46a) \quad (46b)$$

If the pitch angle distribution of bouncing particles is isotropic, then the parallel diffusion coefficient can be approximated by

$$D_{\parallel,\text{inc},b} \approx \int_0^{\mu_c} D_{\parallel,\text{inc},b}(\mu) d\mu = \frac{1}{6}vL\aleph_s^{-2}\mu_c^6, \quad (47)$$

which is energy independent with a constant μ_c . Here we neglect the contribution from $D_{\parallel,\text{inc},b}(\mu)$ at $\mu < \mu_{\text{min},s}$.

We next consider the situation with an anisotropic pitch angle distribution. We follow the similar analysis in Section 3.2 to derive $D_{\parallel,\text{inc},b}$ numerically by using Eqs. (27)-(31). In Eq. (27), we adopt (Eqs. (33) and (34))

$$D_{\mu\mu}(\mu) = D_{\mu\mu,\text{QLT},A} + D_{\mu\mu,\text{QLT},s} \quad (48)$$

to include the gyroresonant scattering by both Alfvén and pseudo-Alfvén modes. Eq. (31) becomes

$$D_{\parallel,\text{inc},b} = \int_0^{\mu_c} D_{\parallel,\text{inc},b}(\mu) f' d\mu, \quad (49)$$

where $D_{\parallel,\text{inc},b}(\mu)$ is given by Eq. (46).

In Fig. 4, we illustrate the numerically calculated $D_{\parallel,\text{inc},b}$ with an anisotropic pitch angle distribution in comparison with the analytical approximation with an isotropic pitch angle distribution (Eq. (47)). The same parameters as in Fig. 2 are used, and the turbulence is considered to be trans-Alfvénic with $\delta B_A = B_0$. Here we also use $\delta B_s = B_0$, i.e., $\aleph_s = 1$. We see that the anisotropic distribution leads to a significantly smaller $D_{\parallel,\text{inc},b}$ than that derived from an isotropic distribution. Fig. 5(a) displays the anisotropic f' caused by the anisotropic pitch-angle scattering for different CR energies. The highly anisotropic scattering originates from the scale-dependent anisotropy of Alfvén and pseudo-Alfvén modes. At a small μ , the gyroresonance with many uncorrelated eddies with the perpendicular eddy size much smaller than r_g makes the scattering inefficient (Chandran 2000a; Yan & Lazarian 2002). Consequently, most particles are concentrated at a small μ .

The more pronounced anisotropy of f' for low-energy CRs is caused by the inner cutoff at k_{max} of turbulent energy spectrum. XL20 found that for the gyroresonance with Alfvén

and pseudo-Alfvén modes, the magnetic fluctuations at

$$k_{\perp p} = \left(\frac{L^{\frac{1}{3}} k_{\parallel,\text{res}}}{8} \right)^{\frac{3}{2}} = 8^{-\frac{3}{2}} k_{\perp,\text{res}} \quad (50)$$

play a dominant role in determining the scattering efficiency. Here the parallel and perpendicular resonant wavenumbers are $k_{\parallel,\text{res}} \approx \Omega/v_{\parallel}$ and $k_{\perp,\text{res}} = L^{\frac{1}{2}} k_{\parallel,\text{res}}^{\frac{3}{2}}$ for trans-Alfvénic turbulence. The former is derived from the resonance condition in Eq. (11). When $k_{\perp p} > k_{\text{max}}$ at a small μ and a low E_{CR} , the scattering becomes ineffective, leading to a more anisotropic f' . As a result, the integral in Eq. (49) is dominated by $D_{\parallel,\text{inc},b}(\mu)$ at a small μ (Eq. (46b)) (see Fig. 5(c)). For the parameters adopted here, the CR energy corresponding to $k_{\perp p} = k_{\text{max}} = 10^{-8} \text{ cm}^{-1}$ and the minimum $\mu = 0.01$ is indicated by the dashed line in Fig. 4, below which the damping of turbulent spectrum has a significant effect on the diffusion of bouncing particles. The enhanced anisotropy due to damping gives rise to more suppressed diffusion.

At higher energies, Eq. (49) is dominated by $D_{\parallel,\text{inc},b}(\mu)$ at a larger μ , where both f' and $D_{\parallel,\text{inc},b}(\mu)$ remain unchanged (Figs. 5(a) and 5(b)), and the resulting $D_{\parallel,\text{inc},b}$ becomes energy independent (Fig. 4). For high-energy CRs, Eq. (49) is again dominated by $D_{\parallel,\text{inc},b}(\mu)$ at a small μ similar to low-energy CRs, but due to the increase of r_g with E_{CR} (Eq. (46b)). At both low- and high-energy ends, $D_{\parallel,\text{inc},b}$ has the energy dependence close to $D_{\parallel,\text{inc},b} \propto E_{\text{CR}}$ as dictated by Eq. (46b).

In the vicinity of a CR source, the initial pitch angle distribution of the injected CRs is important for determining the parallel diffusion of bouncing CRs until they lose the memory about the initial distribution via scattering. Therefore, the CRs closer to the source can have slower diffusion.

We see that even though the pitch-angle scattering is inefficient in incompressible trans-Alfvén MHD turbulence, the bouncing effect due to the presence of pseudo-Alfvén modes significantly suppresses the parallel diffusion of CRs. This result brings a significant changes for the theory of CR diffusion in incompressible MHD turbulence that does not account for the effect of CR reflections from magnetic mirrors, e.g., Chandran (2000a); Yan & Lazarian (2002).

4.2. Super- and sub-Alfvénic turbulence

In the above analysis, we discussed the case of trans-Alfvénic turbulence with $M_A = 1$, or equivalently, $\delta B_A = B_0$. Our analysis can be generalized for both super- and sub-Alfvénic turbulence.

For super-Alfvénic turbulence ($M_A > 1$), the perpendicular superdiffusion (Lazarian & Vishniac 1999; Lazarian 2006; Lazarian & Yan 2014) takes place on scales less than l_A .⁶ For the analysis in Section 4.1 for anisotropic MHD turbulence to be applicable, we use l_A (Eq. (A4)) as the ef-

⁶ On scales larger than l_A , CRs following magnetic field lines undergo isotropic diffusion with the step size equal to l_A (see Brunetti & Lazarian 2007).

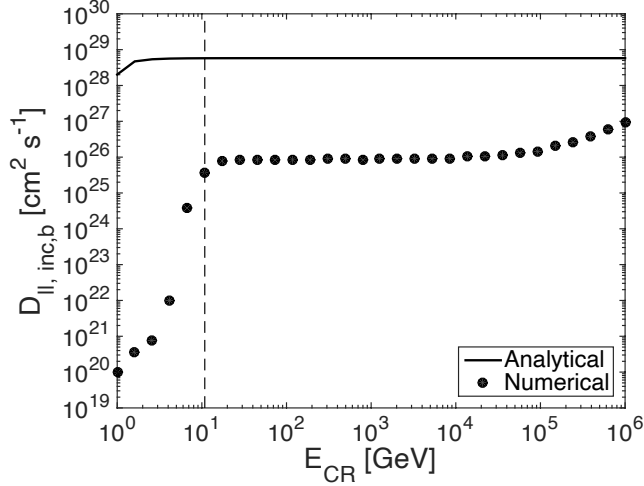


Figure 4. Parallel diffusion coefficient $D_{\parallel, \text{inc}, b}$ of bouncing CRs as a function of CR energy in incompressible MHD turbulence. The numerical and analytical (Eq. (47)) results are obtained using anisotropic and isotropic pitch angle distribution, respectively. The dashed line indicates the energy, below which the diffusion is affected by damping of turbulence.

fective injection scale of turbulence with the injected turbulent velocity equal to V_A . Therefore, after replacing L by l_A , we can still use the expressions in Section 4.1 for describing the parallel diffusion of bouncing particles on scales smaller than l_A in super-Alfvénic turbulence. We note that δB_s in this case should be measured at l_A instead of L .

In sub-Alfvénic turbulence with $M_A < 1$, as we discuss in Appendix A, the so-called weak turbulence (Lazarian & Vishniac 1999; Galtier et al. 2000) exists on scales from L down to $l_{\text{tran}} = LM_A^2$. Strong MHD turbulence is only developed on scales below l_{tran} . In the strong turbulence regime in sub-Alfvénic turbulence, the turbulence scaling is different from that in trans-Alfvénic turbulence, and the turbulent eddies are more elongated, with the elongation depending on M_A (Lazarian & Vishniac 1999). We notice in Appendix A, if we introduce an effective injection scale L_{eff} for sub-Alfvénic turbulence that is given by Eq. (A9), then we can describe the subAlfvénic turbulence at scales less than LM_A^2 as arising from the fictitious driving with the injection scale L_{eff} and injection velocity V_A .

It is larger than the actual injection scale L by a factor of M_A^{-4} . Unlike l_A in super-Alfvénic turbulence, where the transition from isotropic to anisotropic turbulence occurs, L_{eff} does not have a well-defined physical meaning. Its introduction, nevertheless, allows us to generalize the results for trans-Alfvénic turbulence to the strong turbulence regime of sub-Alfvénic turbulence by replacing L used in Section 4.1 by L_{eff} . δB_s in this case should be measured at L_{eff} , and it is related to the magnetic perturbation $\delta B_{s, L}$ of pseudo-Alfvén modes at L by

$$\delta B_s = \delta B_{s, L} M_A^{-2}. \quad (51)$$

In Table 1, we summarize the parameters introduced for generalizing the results on diffusion of bouncing particles in trans-Alfvénic turbulence to super- and sub-Alfvénic turbulence.

5. AVERAGED PARALLEL DIFFUSION COEFFICIENTS FOR ALL PARTICLES

The analysis on the parallel diffusion of bouncing particles in Sections 3 and 4 can be applied to the bouncing CRs near a CR source. On scales much larger than the mean free paths of both bouncing and non-bouncing particles, we need to consider their exchange and the isotropization of pitch angle distribution due to scattering. In this case we define an averaged parallel diffusion coefficient for all particles as

$$D_{\parallel, \text{tot}} \approx \alpha D_{\parallel, b} + (1 - \alpha) D_{\parallel, nb}, \quad (52)$$

where

$$\alpha = \frac{\tau_b}{\tau_b + \tau_{nb}}, \quad 1 - \alpha = \frac{\tau_{nb}}{\tau_b + \tau_{nb}}, \quad (53)$$

τ_b and τ_{nb} represent the times for particles to stay in the bouncing state and non-bouncing state, respectively. As a simple estimate, we have

$$\tau_b \approx \frac{\mu_c^2}{D_{\mu\mu}}, \quad \tau_{nb} \approx \frac{1 - \mu_c^2}{D_{\mu\mu}} \quad (54)$$

to account for the diffusion in pitch angle by scattering and the resulting transition from bouncing (non-bouncing) to non-bouncing (bouncing) particles. For the weakly anisotropic pitch angle distribution under consideration, we can use $D_{\mu\mu}$ at μ_c in the above expression as an approximation. Therefore, Eq. (52) can be rewritten as

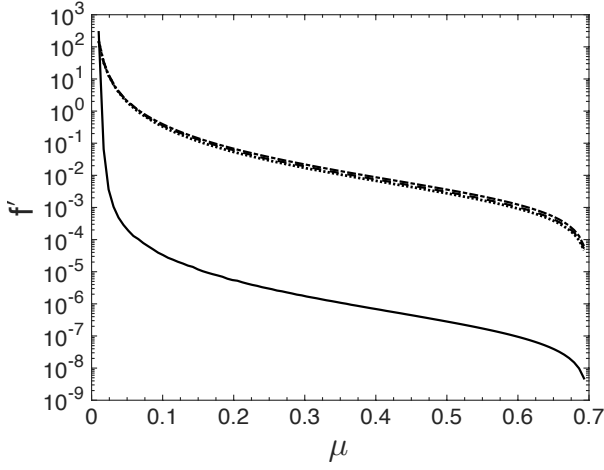
$$D_{\parallel, \text{tot}} \approx \mu_c^2 D_{\parallel, b} + (1 - \mu_c^2) D_{\parallel, nb}. \quad (55)$$

Over a timescale T much longer than τ_b and τ_{nb} , the mean squared displacement of CRs in the bouncing state is

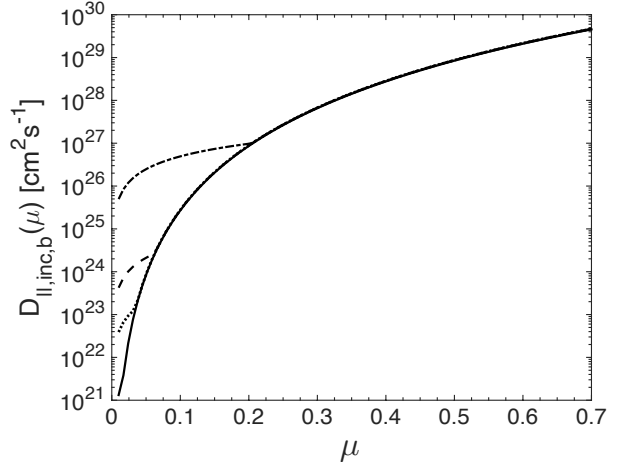
$$\Delta_b^2 = D_{\parallel, b} \alpha T, \quad (56)$$

and the mean squared displacement of CRs in the non-bouncing state is

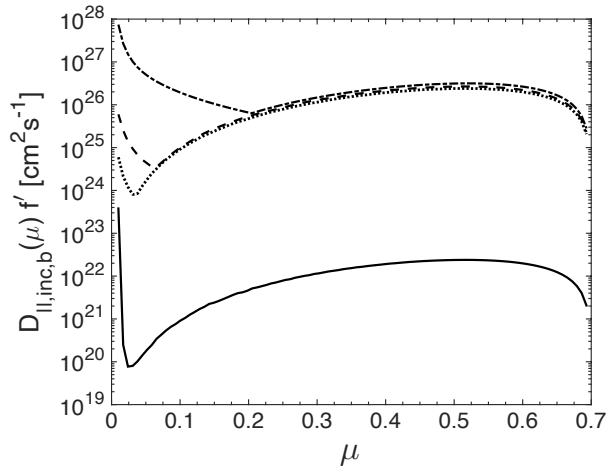
$$\Delta_{nb}^2 = D_{\parallel, nb} (1 - \alpha) T. \quad (57)$$



(a)



(b)



(c)

Figure 5. (a) Normalized particle distribution function f' , (b) μ -dependent parallel diffusion coefficient $D_{\parallel,inc,b}(\mu)$, and (c) $D_{\parallel,inc,b}(\mu)f'$ vs. μ for 4 GeV (solid line), 10^2 GeV (dotted line), 10^3 GeV (dashed line), and 10^5 GeV (dash-dotted line) bouncing CRs in incompressible MHD turbulence.

]

Table 1. [

	L_{eff}	δB_s at L_{eff}	Range of length scales
Super-Alfvénic turbulence ($M_A > 1$)	$l_A = LM_A^{-3}$	δB_s at l_A	$< l_A$
Sub-Alfvénic turbulence ($M_A < 1$)	LM_A^{-4}	$\delta B_{s,L} M_A^{-2}$	$< LM_A^2$

The total mean squared displacement $\Delta_{\text{tot}}^2 = \Delta_b^2 + \Delta_{nb}^2$ during T corresponds to a total diffusion coefficient

$$D_{\parallel,\text{tot}} = \frac{\Delta_{\text{tot}}^2}{T} \approx \alpha D_{\parallel,b} + (1 - \alpha) D_{\parallel,nb}, \quad (58)$$

which recovers Eq. (52). In the case with $D_{\parallel,b} \ll D_{\parallel,nb}$, $D_{\parallel,\text{tot}}$ can be dominated by the diffusion of non-bouncing particles, that is,

$$D_{\parallel,\text{tot}} \approx (1 - \alpha) D_{\parallel,nb}. \quad (59)$$

It is different from the parallel diffusion coefficient in XL20 by a factor of $1 - \alpha$.

5.1. Compressible MHD turbulence with fast modes dominating magnetic fluctuations

In Section 3, we derived the parallel diffusion coefficients of bouncing and non-bouncing particles separately (see Fig. 3). Based on these calculations and by using Eq. (55), here we present $D_{\parallel,f,\text{tot}}$ for all particles interacting with fast modes in compressible MHD turbulence, as shown in Fig. 6. By comparing Fig. 6 with Fig. 3, we see that as $D_{\parallel,f,nb}$ is considerably larger than $D_{\parallel,f,b}$ for the range of E_{CR} under consideration, the resulting $D_{\parallel,f,\text{tot}}$ is determined by $D_{\parallel,f,nb}$ alone and slightly smaller than $D_{\parallel,f,nb}$ with the increase of μ_c toward high energies. We note that unlike $D_{\parallel,f}$ usually defined for pitch-angle scattering that corresponds to the change of pitch angle by 90° , $D_{\parallel,f,nb}$ corresponds to a smaller change of pitch angle and is smaller than $D_{\parallel,f}$ with $\mu_c = 0$ (see Eq. (32)).

5.2. Compressible MHD turbulence with a varying fraction of fast modes

In realistic astrophysical media, the energy fraction of fast modes depends on the driving condition of turbulence and plasma β (see Section 2.1).

In the presence of both fast and slow modes, the ratio between their bouncing rates (Eqs (16) and (40)) is

$$\frac{\Gamma_{b,f}}{\Gamma_{b,s}} = \frac{\delta B_f^4}{B_0^2 \delta B_s^2} \mu^{-4}, \quad (60)$$

when $\mu > \mu_{\text{min},f}$ and $\mu > \mu_{\text{min},s}$. We use the larger one, i.e., $\max[\Gamma_{b,f}, \Gamma_{b,s}]$, as the bouncing rate. In the case of $\delta B_f \sim \delta B_s \sim B_0$, there is always $\Gamma_{b,f} > \Gamma_{b,s}$ and fast modes dominate bouncing.

In Fig. 7, we consider the parallel diffusion coefficients of bouncing and non-bouncing particles in trans-Alfvénic turbulence with a varying fraction of fast modes, and we adopt an isotropic pitch angle distribution. \aleph_s is fixed at 0.5 to address the role of fast modes in affecting the diffusion coefficients.

(a) $\delta B_f = 0$. In the limit case of incompressible MHD turbulence with $\delta B_f = 0$ (Fig. 7(a)), scattering is inefficient and μ_c is given by Eq. (44) (see Fig. 8). $D_{\parallel,b}$ is consistent with Eq. (47). $D_{\parallel,nb}$ is

$$D_{\parallel,nb} = \frac{v^2}{4} \int_{\mu_c}^1 d\mu \frac{(1 - \mu^2)^2}{D_{\mu\mu}(\mu)}, \quad (61)$$

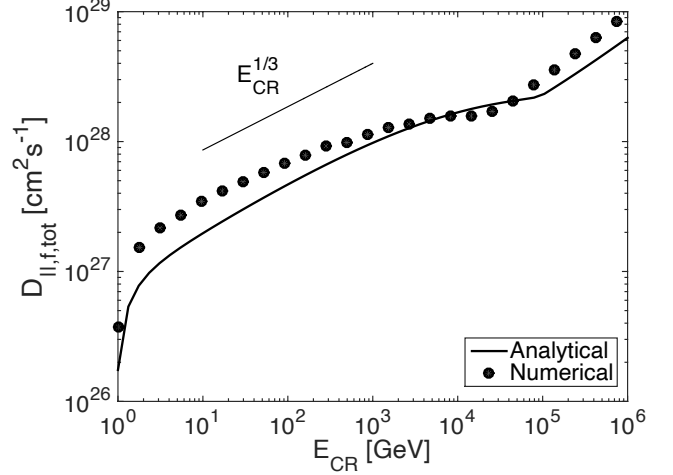


Figure 6. Total parallel diffusion coefficient $D_{\parallel,f,\text{tot}}$ as a function of E_{CR} in compressible MHD turbulence with magnetic fluctuations dominated by fast modes.

where $D_{\mu\mu}(\mu)$ is given by Eq. (48). As both $D_{\mu\mu,\text{QLT},A}$ and $D_{\mu\mu,\text{QLT},s}$ have energy dependance as $\propto E_{\text{CR}}^{3/2}$ (XL20), the resulting $D_{\parallel,nb}$ decreases with increasing energy following $\propto E_{\text{CR}}^{-3/2}$. Because the turbulence anisotropy is weaker toward larger length scales, higher-energy CRs are more efficiently scattered and have smaller $D_{\parallel,nb}$.

(b) $\delta B_f = 0.01 B_0$. In compressible MHD turbulence, we consider the scattering rate with contributions from all three modes,

$$\Gamma_{s,\text{tot}} = \frac{2(D_{\mu\mu,\text{QLT},A} + D_{\mu\mu,\text{QLT},s} + D_{\mu\mu,\text{QLT},f})}{\mu^2}. \quad (62)$$

When there is a tiny fraction of fast modes with $\delta B_f \ll B_0$ (see Fig. 7(b)), the scattering of low-energy CRs is dominated by fast modes despite their negligible energy fraction. With a constant μ_c (Fig. 8), $D_{\parallel,nb}$ determined by $D_{\parallel,f,nb}$ increases with energy as $\propto E_{\text{CR}}^{0.5}$ (see Eq. (32)). The scattering of higher-energy CRs is taken over by Alfvén and slow modes. For bouncing CRs, $D_{\parallel,b}$ is determined by slow modes and is the same as that in the incompressible turbulence.

(c) $\delta B_f = 0.1 B_0$. When we further increase the fraction of fast modes (Fig. 7(c)), scattering is dominated by fast modes

for most energies, resulting in the energy dependence of μ_c until it reaches its maximum value (Fig. 8). With increasing μ_c , $D_{\parallel,nb}$ has a weaker dependence on E_{CR} than $\propto E_{CR}^{0.5}$ (Eq. (32)) for low-energy CRs. For bouncing of CRs, although $\Gamma_{b,f}$ is larger than $\Gamma_{b,s}$ at a small μ for low-energy CRs (Eq. (60)), $D_{\parallel,b}$ is still determined by slow modes for most energies and Eq. (47) applies.

(d) $\delta B_f = 0.5B_0$. With a large fraction of fast modes, fast modes dominate both scattering and bouncing. $D_{\parallel,nb}$ (see Eq. (32)) approximately follows $\propto E_{CR}^{1/3}$ (see Fig. 7(d)). $D_{\parallel,b}$ in this case is given by Eq. (24) and is close to $\propto E_{CR}$.

The thick solid lines in all cases represent the averaged $D_{\parallel,tot}$ (Eq. (55)). It is basically determined by $D_{\parallel,nb}$ as $D_{\parallel,tot}$ is considerably larger than $D_{\parallel,b}$.

Based on the above results, our main findings are:

(i) The difference between $D_{\parallel,nb}$ dominated by incompressible modes and fast modes comes from not only the different slopes of turbulent energy spectra, but also the anisotropy of turbulence. The scale-dependent turbulence anisotropy in the former case results in a decreasing $D_{\parallel,nb}$ with increasing E_{CR} .

(ii) Even with a small fraction of fast modes, scattering becomes much more efficient than that in incompressible turbulence.

(iii) With an energy-dependent μ_c , $D_{\parallel,nb}$ dominated by fast modes has a weaker dependence on E_{CR} than the case with a constant μ_c .

(iv) With a non-zero μ_c and a factor $1 - \alpha$, $D_{\parallel,nb}$ is in general smaller than the parallel diffusion coefficient for gyroresonant scattering with $\mu_c = 0$ and $\alpha = 0$.

(v) The maximum $D_{\parallel,b}$ depends on the maximum μ_c , which is determined by the amplitude of magnetic fluctuations (δB_s or δB_f) of the modes that dominate bouncing.

(vi) The dependence of $D_{\parallel,tot}$ on E_{CR} is non-universal.

6. DISCUSSION

The paradigm of CR propagation has significantly shifted over the past two decades. First of all, the fast modes of MHD turbulence were identified as the major scattering agent for diffusion of CRs with $r_g \ll L$ in the interstellar medium (Yan & Lazarian 2002, 2003). On the contrary, the Alfvén and slow modes, which were traditionally considered for CR diffusion, were found to be very inefficient in scattering (Chandran 2000a; Yan & Lazarian 2002). Therefore, it was believed that, when the CR streaming instability is inefficient (see Yan & Lazarian 2002; Farmer & Goldreich 2004; Lazarian 2016) and fast modes are absent, CRs propagate ballistically along magnetic field lines without scattering.⁷

In this work, we find a new diffusion mechanism for CRs that encounter magnetic compressions induced by slow (pseudo-Alfvén) and fast modes. This bouncing-related parallel diffusion of CRs can take place even in incompress-

ible MHD turbulence and cause slower diffusion than that induced by scattering in both incompressible and compressible MHD turbulence. The inefficient diffusion of bouncing CRs near the CR source provides a possible explanation for the small diffusion coefficient of high-energy electrons and positrons within pulsar wind nebulae suggested by recent observations (e.g., Abeysekera et al. 2017; Huang et al. 2018).

In addition, the bouncing of CRs also affects the parallel diffusion associated with scattering. In the presence of bouncing, the scattering even in the quasilinear approximation does not face the 90° problem (Noerdlinger 1968; Kulsrud & Pearce 1969; Felice & Kulsrud 2001), and also the resulting mean free path corresponds to the pitch angle change over a smaller range $[\mu_c, 1]$, as pointed out by Cesarsky & Kulsrud (1973). In XL20, we derived the parallel diffusion coefficient for scattering by fast modes in the presence of bouncing. With an energy-dependent μ_c , the diffusion coefficient has an energy dependence close to $\propto E^{1/3}$ instead of $\propto E^{0.5}$. In earlier studies (e.g., Ptuskin et al. 2006), the energy dependence $\propto E^{1/3}$ of diffusion coefficient is only expected for the Kolmogorov spectrum of turbulence, but the Alfvén and slow modes with the Kolmogorov spectrum are incapable of scattering. Our finding provides a solution to this theoretical problem.

Furthermore, the bouncing of CRs also brings a new acceleration mechanism. The bouncing does not change a particle's pitch angle if the magnetic mirrors are static. When encountering moving magnetic mirrors in MHD turbulence, CRs undergo the second order Fermi acceleration with the stochastic increase of parallel momentum p_{\parallel} and μ . Together with other acceleration mechanisms, e.g., TTD, that also cause the stochastic increase of μ , the bouncing can enhance the diffusion in μ and the transition of particles from bouncing to non-bouncing state. This new acceleration mechanism and its implications will be studied in our future work.

The diffusive propagation of CRs plays an important role in the first order Fermi acceleration processes at shocks (e.g., Schlickeiser & Oppotsch 2017) and in magnetic reconnection regions (de Gouveia dal Pino & Lazarian 2005; Lazarian 2005; Kowal et al. 2012). Both the perpendicular superdiffusion and the parallel diffusion resulting from bouncing and scattering should be taken into account when studying the acceleration of CRs (see, e.g., Lazarian & Yan 2014).

In this work we did not consider the effect of instabilities on scattering of relatively low-energy CRs. We note that the CR streaming instability can be suppressed in the galactic disk through both ion-neutral collisional damping (Kulsrud & Pearce 1969; Xu et al. 2016; Krumholz et al. 2020) and the interaction with Alfvénic turbulence (Yan & Lazarian 2002; Farmer & Goldreich 2004; Lazarian 2016). However, it can give rise to efficient scattering in the galactic halo and make CRs return to the disk (Lazarian 2016). As both bouncing and streaming instability can cause inefficient diffusion, their relative importance in various environments deserves further investigation.

⁷ We note that in super-Alfvénic turbulence, CRs that follow the tangled magnetic fields without scattering have an effective mean free path given by l_A (Brunetti & Lazarian 2007).

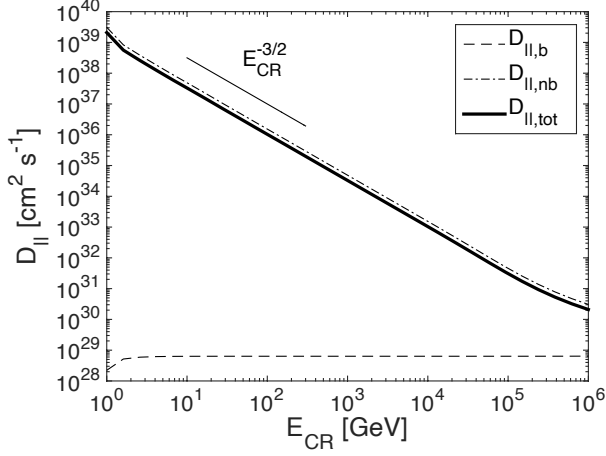
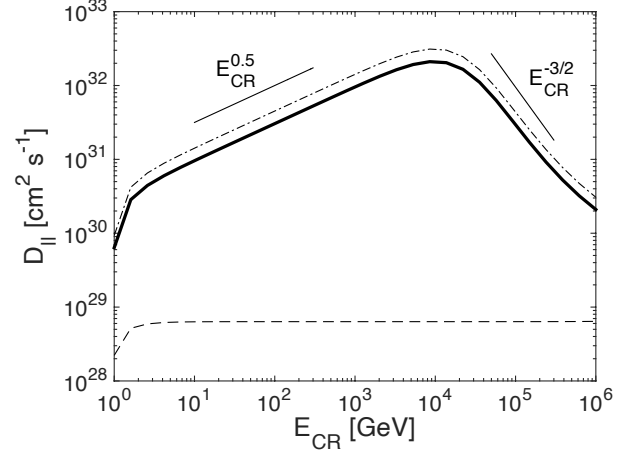
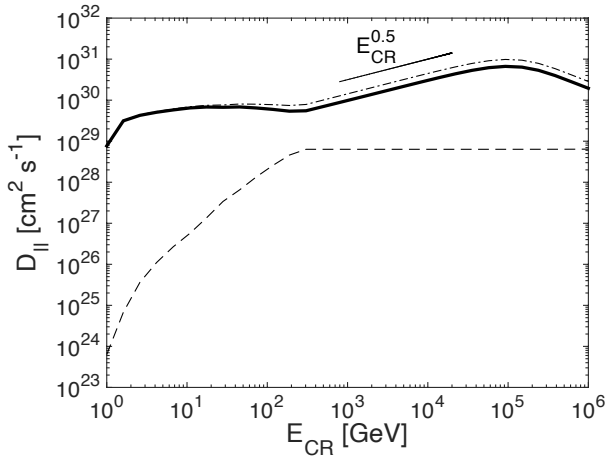
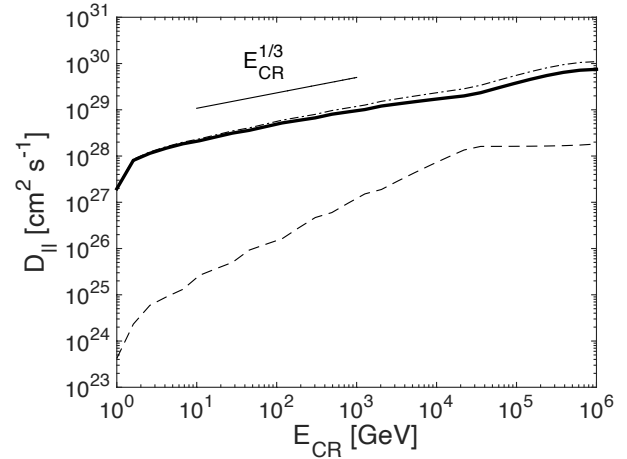
(a) $\delta B_f/B_0 = 0, N_s = 0.5$ (b) $\delta B_f/B_0 = 0.01, N_s = 0.5$ (c) $\delta B_f/B_0 = 0.1, N_s = 0.5$ (d) $\delta B_f/B_0 = 0.5, N_s = 0.5$

Figure 7. Parallel diffusion coefficients of bouncing particles $D_{\parallel,b}$, non-bouncing particles $D_{\parallel,nb}$, and the averaged parallel diffusion coefficient $D_{\parallel,tot}$ in MHD turbulence with different fractions of fast modes. The pitch angle distribution is assumed to be isotropic.

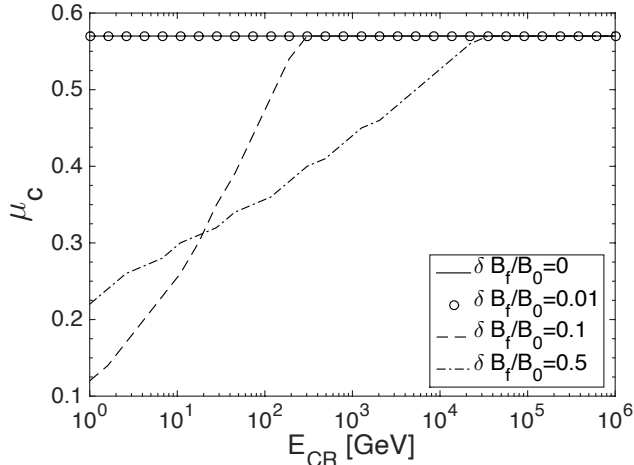


Figure 8. μ_c vs. E_{CR} for different fractions of fast modes.

We note that fast modes can be subject to severe damping especially in partially ionized interstellar phases (Xu et al. 2015, 2016). The effect of damping of fast modes on scattering of CRs has been addressed in earlier studies, e.g., Yan & Lazarian (2004); Xu et al. (2016); Xu & Lazarian (2018). We did not consider the damping of fast modes in this work but caution that it may have a significant effect on bouncing of CRs in the partially ionized ISM.

7. SUMMARY

The perpendicular superdiffusion of CRs originates from the superdiffusion of magnetic fields induced by Alfvénic turbulence. This effect makes the trapping of CR within mag-

netic bottles improbable. Instead, CRs bounce among different magnetic mirrors and move diffusively parallel to the magnetic field. As a result, both bouncing and pitch-angle scattering contribute to the parallel diffusion. The former governs the parallel diffusion of CRs at large pitch angles with $\mu < \mu_c$, and the latter is dominant at $\mu > \mu_c$, where μ_c corresponds to the balance between bouncing and scattering. The two diffusion processes interact with each other through exchanging CRs via the pitch angle diffusion.

In the case when fast modes dominate both scattering and bouncing, μ_c increases with E_{CR} . As a result, the diffusion coefficient for scattering by fast modes has a weaker dependence on E_{CR} compared to the case without bouncing, i.e., $\mu_c = 0$. It is not an exact power law function of E_{CR} , but can be approximated by $\propto E_{CR}^{1/3}$. The scaling $\propto E_{CR}^{1/3}$ is expected for isotropic turbulence with the Kolmogorov spectrum and is applied to explaining CR observations (e.g., Blasi et al. 2012). However, the scattering by Alfvén and slow modes with the Kolmogorov spectrum is inefficient and the resulting diffusion coefficient depends on E_{CR} as $\propto E_{CR}^{-3/2}$ due to the scale-dependent turbulence anisotropy. Our finding provides the physical justification for the commonly used energy scaling of diffusion coefficient.

With the bouncing of CRs taken into account, the 90° problem of quasilinear gyroresonant scattering can be solved. Moreover, as the mean free path of bouncing CRs is determined by the size of compressive magnetic fluctuations, which cannot exceed the driving scale of turbulence, the corresponding diffusion is inefficient without invoking efficient scattering by fast modes. The energy scaling of the diffusion coefficient of bouncing CRs depends on the anisotropy of pitch angle distribution and the energy dependence of μ_c .

In the vicinity of a CR source, the injected CRs can have an anisotropic pitch angle distribution. Note that the damping of turbulence can also affect the anisotropic distribution. If there are more particles at larger pitch angles, the diffusion of bouncing CRs can be further suppressed.

For the galactic environment with a nearly uniform and isotropic distribution of CRs, the average diffusion coefficient for both bouncing and non-bouncing CRs is usually determined by the diffusion coefficient of the latter, as it is larger than that of bouncing CRs. Its energy scaling can be non-universal, depending on the properties of interstellar turbulence.

APPENDIX

A. BASIC SCALINGS OF MHD TURBULENCE

A.1. Scalings of incompressible MHD turbulence

MHD turbulence is a major agent determining the dynamics of CRs. The turbulence in magnetized media in typical astrophysical settings is injected at the scale L with the injection velocity V_L , and the turbulent energy then cascades down to smaller scales. If the injection happens with $V_L > V_A$, where V_A is the Alfvén speed, this is the case of super-Alfvénic turbulence. If $V_L < V_A$, the turbulence is sub-Alfvénic. The ratio $M_A = V_L/V_A$ is the Alfvén Mach number. $M_A = 1$ corresponds to the trans-Alfvénic turbulence.

Note that we consider turbulence as a result of energy cascade. Therefore the Alfvén waves excited by CR instabilities, e.g. streaming instabilities (see [Farmer & Goldreich 2004](#)), gyro-resonance instabilities (see [Lazarian & Beresnyak 2006](#)), are not classified as turbulence.

The theory of trans-Alfvénic turbulence was developed by [Goldreich & Sridhar \(1995\)](#) (henceforth GS95) in the global system of reference with respect to the mean magnetic field. [Lazarian & Vishniac \(1999\)](#) (henceforth LV99) presented an alternative way to derive the GS95 theory based on the theory of turbulent reconnection of magnetic fields. More importantly, they found that the GS95 theory is only valid in the “local system of reference” with respect to the local mean magnetic field averaged over the length scale of interest, as confirmed by numerical simulations ([Cho & Vishniac 2000](#); [Maron & Goldreich 2001](#); [Cho et al. 2002](#)). According to the LV99 theory, magnetic reconnection takes place within one eddy turnover time, which allows the turbulent motions to mix up magnetic fields without bending them. The unconstrained eddy rotation occurs in the system of reference of the local magnetic field averaged over the eddy scale, and the eddy is aligned with the local magnetic field. The direction of the local magnetic field averaged over a small scale can differ significantly from the global mean magnetic field direction averaged over a large scale.

The turbulent cascade in the direction perpendicular to the local magnetic field remains Kolmogorov-like with

$$v_l \approx V_A \left(\frac{l_\perp}{L} \right)^{1/3}, \quad (\text{A1})$$

where it is taken into account that $V_L = V_A$ for trans-Alfvénic turbulence, v_l is the turbulent velocity at l_\perp , and l_\perp is the perpendicular size of a turbulent eddy. The eddy rotation perpendicular to the local magnetic field induces Alfvénic perturbation that propagates along the magnetic field with the speed V_A . The timescale of this perturbation l_\parallel/V_A should be equal to the eddy turnover time l_\perp/v_l . The corresponding relation between the parallel and perpendicular sizes of the eddy

$$\frac{l_\parallel}{V_A} \approx \frac{l_\perp}{v_l}, \quad (\text{A2})$$

was termed as the “critical balance” in GS95. By combining Eq. (A1) and Eq. (A2), one can obtain the scale-dependent anisotropy of trans-Alfvénic turbulence

$$l_\parallel \approx L \left(\frac{l_\perp}{L} \right)^{2/3}. \quad (\text{A3})$$

Smaller eddies are more elongated along the local magnetic field. Note that Eqs. (A1) and (A3) should be understood in the statistical sense. They represent the scaling relations between the most probable values of the quantities involved. For instance, on the basis of numerical simulations, [Cho et al. \(2002\)](#) provided an analytical fit for the detailed distribution function describing the probability of finding a l_\perp at a given l_\parallel . This was used later in [Yan & Lazarian \(2002, 2004\)](#) and subsequent studies on CR scattering.

For super-Alfvénic turbulence injected with $M_A > 1$, the magnetic field is of marginal importance at L . The super-Alfvénic turbulence is initially hydrodynamic-like with the isotropic Kolmogorov energy spectrum. With the decrease of turbulent velocity along the energy cascade, $v_l \sim V_L (l/L)^{1/3}$, where v_l is the turbulent velocity at the length scale l , the effect of magnetic field becomes more and more manifested. Eventually, at the scale ([Lazarian 2006](#))

$$l_A = LM_A^{-3}, \quad (\text{A4})$$

v_l becomes equal to V_A , and the turbulence becomes fully magnetohydrodynamic. To describe the MHD cascade on scales less than l_A in super-Alfvénic turbulence, L in Eqs. (A1) and (A3) should be replaced by l_A .

For sub-Alfvénic turbulence with $M_A < 1$, it was shown in LV99 that at L the turbulence is *weak*, and the parallel scale of wave packets remains unchanged, i.e. $l_\parallel = L$. The scaling obtained in LV99 for the weak turbulence under the assumption of the isotropic turbulence driven at L is

$$v_l \approx V_L \left(\frac{l_\perp}{L} \right)^{1/2}, \quad (\text{A5})$$

and this result was supported by the subsequent study by [Galtier et al. \(2000\)](#). With the decrease of l_\perp , the intensity of interactions of Alfvénic perturbations increases. At a scale (LV99)

$$l_{\text{tran}} \approx LM_A^2, \quad (\text{A6})$$

where $M_A < 1$, the turbulence gets strong. For the sub-Alfvénic MHD turbulence at $l < l_{\text{tran}}$, LV99 derived the relations

$$v_l \approx V_L \left(\frac{l_\perp}{L} \right)^{1/3} M_A^{1/3}, \quad (\text{A7})$$

and

$$l_{\parallel} \approx L \left(\frac{l_{\perp}}{L} \right)^{2/3} M_A^{-4/3}, \quad (\text{A8})$$

which at $M_A = 1$ can recover the relations in Eqs. (A1) and (A3) for trans-Alfvénic turbulence.

To generalize our analysis for diffusion of bouncing particles in trans-Alfvénic turbulence to super- and sub-Alfvénic turbulence, we introduce the following effective injection scales.

(1) Super-Alfvénic turbulence. As discussed above, the super-Alfvénic turbulence at $l < l_A$ is equivalent to the trans-Alfvénic turbulence injected at l_A . So by using l_A as the effective injection scale to replace L in trans-Alfvénic turbulence, the results derived for trans-Alfvénic are still applicable to super-Alfvénic on scales less than l_A .

(2) Sub-Alfvénic turbulence. By introducing an effective injection scale

$$L_{\text{eff}} = L M_A^{-4}, \quad (\text{A9})$$

Eqs. (A7) and (A8) can be rewritten as

$$v_l \approx V_A \left(\frac{l_{\perp}}{L_{\text{eff}}} \right)^{1/3}, \quad (\text{A10})$$

and

$$l_{\parallel} \approx L_{\text{eff}} \left(\frac{l_{\perp}}{L_{\text{eff}}} \right)^{2/3}, \quad (\text{A11})$$

which take the same forms as Eqs. (A1) and (A3) with L replaced by L_{eff} . Therefore, by using L_{eff} instead of L , the expressions for trans-Alfvénic turbulence can be applied to sub-Alfvénic turbulence on scales less than l_{tran} .

A.2. Magnetic compressions in MHD turbulence

The magnetic mirroring effect arise from the magnetic compressions in MHD turbulence, which are associated with slow and fast modes. We use the term “modes” rather than “waves”, as the nonlinear interactions intrinsic to the turbulent cascade make the properties of magnetic fluctuations different from the properties of linear waves. We stress that the compression of magnetic field can also occur in incompressible MHD turbulence. The incompressible limit of slow modes, i.e., pseudo-Alfvén modes (see GS95), is a typical example for turbulent compression of magnetic field in an incompressible medium.

It was pointed out in GS95 that Alfvén modes impose their scaling on the pseudo-Alfvén modes. With a finite compressibility, slow modes also follow the same scaling as Alfvén modes. This property was discussed in Lithwick & Goldreich (2001) and confirmed numerically by Cho & Lazarian (2002b, 2003). As discussed above, the anisotropic scaling of slow modes is defined and should be measured in the local system of reference. For bouncing CRs that interact with the magnetic compression generated by slow modes, they only feel the local magnetic field averaged over the scale of the magnetic compression. When describing the gyroresonant scattering of non-bouncing CRs, they also only feel the local magnetic field averaged over the scale comparable to r_L . The QLT for scattering is formally only applicable to infinitesimally small magnetic perturbations. In the local system of reference, CRs only interact with the small magnetic fluctuations on small scales, while the large fluctuations on large scales are not involved. This extends the applicability of the QLT.

Fast modes are different from Alfvén and slow modes. Their evolution is not related to the local system of reference. Therefore, the traditional wave representation is applicable to fast modes. The scaling of fast modes is somewhat less certain. The theoretical considerations in LG01 for high- β plasma and in Cho & Lazarian (2002b, 2003) for low- β plasma suggested the “isotropic” energy spectrum of fast modes with $k^{-3/2}$ similar to the acoustic-type turbulence. However, the simulations in Kowal & Lazarian (2010) indicated a steeper spectrum close to k^{-2} for fast modes. This discrepancy may be attributed to the effect of shocks in the latter study.

REFERENCES

- Abeysekara, A. U., Albert, A., Alfaro, R., et al. 2017, *Science*, 358, 911, doi: [10.1126/science.aan4880](https://doi.org/10.1126/science.aan4880)
- Amato, E., & Casanova, S. 2021, *Journal of Plasma Physics*, 87, 845870101, doi: [10.1017/S0022377821000064](https://doi.org/10.1017/S0022377821000064)
- Beresnyak, A. 2013, *ApJL*, 767, L39, doi: [10.1088/2041-8205/767/2/L39](https://doi.org/10.1088/2041-8205/767/2/L39)
- . 2014, *ApJL*, 784, L20, doi: [10.1088/2041-8205/784/2/L20](https://doi.org/10.1088/2041-8205/784/2/L20)
- Beresnyak, A., & Lazarian, A. 2019, *Turbulence in Magnetohydrodynamics*
- Blasi, P., Amato, E., & Serpico, P. D. 2012, *PhRvL*, 109, 061101, doi: [10.1103/PhysRevLett.109.061101](https://doi.org/10.1103/PhysRevLett.109.061101)
- Brunetti, G., & Jones, T. W. 2014, *International Journal of Modern Physics D*, 23, 1430007, doi: [10.1142/S0218271814300079](https://doi.org/10.1142/S0218271814300079)

- Brunetti, G., & Lazarian, A. 2007, *MNRAS*, 378, 245, doi: [10.1111/j.1365-2966.2007.11771.x](https://doi.org/10.1111/j.1365-2966.2007.11771.x)
- Budker, G. I. 1959, in *Plasma Physics and the Problem of Controlled Thermonuclear Reactions*, Ed. by M. A. Leontovich (Pergamon, New York), Vol. 1
- Cesarsky, C. J., & Kulsrud, R. M. 1973, *ApJ*, 185, 153
- Chandran, B. D. G. 2000a, *Physical Review Letters*, 85, 4656, doi: [10.1103/PhysRevLett.85.4656](https://doi.org/10.1103/PhysRevLett.85.4656)
- Chandran, B. D. G. 2000b, *ApJ*, 529, 513, doi: [10.1086/308232](https://doi.org/10.1086/308232)
- Cho, J., & Lazarian, A. 2002a, *ApJL*, 575, L63, doi: [10.1086/342722](https://doi.org/10.1086/342722)
- . 2002b, *Physical Review Letters*, 88, 245001, doi: [10.1103/PhysRevLett.88.245001](https://doi.org/10.1103/PhysRevLett.88.245001)
- . 2003, *MNRAS*, 345, 325, doi: [10.1046/j.1365-8711.2003.06941.x](https://doi.org/10.1046/j.1365-8711.2003.06941.x)
- Cho, J., Lazarian, A., & Timbie, P. T. 2012, *ApJ*, 749, 164, doi: [10.1088/0004-637X/749/2/164](https://doi.org/10.1088/0004-637X/749/2/164)
- Cho, J., Lazarian, A., & Vishniac, E. T. 2002, *ApJ*, 564, 291, doi: [10.1086/324186](https://doi.org/10.1086/324186)
- Cho, J., & Vishniac, E. T. 2000, *ApJ*, 539, 273, doi: [10.1086/309213](https://doi.org/10.1086/309213)
- de Gouveia dal Pino, E. M., & Lazarian, A. 2005, *A&A*, 441, 845, doi: [10.1051/0004-6361:20042590](https://doi.org/10.1051/0004-6361:20042590)
- Demidem, C., Lemoine, M., & Casse, F. 2020, *PhRvD*, 102, 023003, doi: [10.1103/PhysRevD.102.023003](https://doi.org/10.1103/PhysRevD.102.023003)
- Evoli, C., & Yan, H. 2014, *ApJ*, 782, 36, doi: [10.1088/0004-637X/782/1/36](https://doi.org/10.1088/0004-637X/782/1/36)
- Eyink, G., Vishniac, E., Lalescu, C., et al. 2013, *Nature*, 497, 466, doi: [10.1038/nature12128](https://doi.org/10.1038/nature12128)
- Eyink, G. L., Lazarian, A., & Vishniac, E. T. 2011, *ApJ*, 743, 51, doi: [10.1088/0004-637X/743/1/51](https://doi.org/10.1088/0004-637X/743/1/51)
- Farmer, A. J., & Goldreich, P. 2004, *ApJ*, 604, 671, doi: [10.1086/382040](https://doi.org/10.1086/382040)
- Felice, G. M., & Kulsrud, R. M. 2001, *ApJ*, 553, 198, doi: [10.1086/320651](https://doi.org/10.1086/320651)
- Fermi, E. 1949, *Physical Review*, 75, 1169, doi: [10.1103/PhysRev.75.1169](https://doi.org/10.1103/PhysRev.75.1169)
- Fisk, L. A., Goldstein, M. L., Klimas, A. J., & Sandri, G. 1974, *ApJ*, 190, 417, doi: [10.1086/152893](https://doi.org/10.1086/152893)
- Forman, M. A., Wicks, R. T., & Horbury, T. S. 2011, *ApJ*, 733, 76, doi: [10.1088/0004-637X/733/2/76](https://doi.org/10.1088/0004-637X/733/2/76)
- Gabici, S., Evoli, C., Gaggero, D., et al. 2019, arXiv e-prints, arXiv:1903.11584. <https://arxiv.org/abs/1903.11584>
- Galtier, S., Nazarenko, S. V., Newell, A. C., & Pouquet, A. 2000, *Journal of Plasma Physics*, 63, 447, doi: [10.1017/S0022377899008284](https://doi.org/10.1017/S0022377899008284)
- Giacalone, J., & Jokipii, J. R. 1999, *ApJ*, 520, 204, doi: [10.1086/307452](https://doi.org/10.1086/307452)
- Goldreich, P., & Sridhar, S. 1995, *ApJ*, 438, 763, doi: [10.1086/175121](https://doi.org/10.1086/175121)
- Guo, F., & Oh, S. P. 2008, *MNRAS*, 384, 251, doi: [10.1111/j.1365-2966.2007.12692.x](https://doi.org/10.1111/j.1365-2966.2007.12692.x)
- Holguin, F., Ruszkowski, M., Lazarian, A., Farber, R., & Yang, H. Y. K. 2019, *MNRAS*, 490, 1271, doi: [10.1093/mnras/stz2568](https://doi.org/10.1093/mnras/stz2568)
- Horbury, T. S., Forman, M., & Oughton, S. 2008, *PhRvL*, 101, 175005, doi: [10.1103/PhysRevLett.101.175005](https://doi.org/10.1103/PhysRevLett.101.175005)
- Huang, Z.-Q., Fang, K., Liu, R.-Y., & Wang, X.-Y. 2018, *ApJ*, 866, 143, doi: [10.3847/1538-4357/aadfed](https://doi.org/10.3847/1538-4357/aadfed)
- Ipavich, F. M. 1975, *ApJ*, 196, 107, doi: [10.1086/153397](https://doi.org/10.1086/153397)
- Jokipii, J. R. 1966, *ApJ*, 146, 480, doi: [10.1086/148912](https://doi.org/10.1086/148912)
- . 1971, *Reviews of Geophysics and Space Physics*, 9, 27, doi: [10.1029/RG009i001p00027](https://doi.org/10.1029/RG009i001p00027)
- Klepach, E. G., & Ptuskin, V. S. 1995, *Astronomy Letters*, 21, 411
- Kóta, J., & Jokipii, J. R. 2000, *ApJ*, 531, 1067, doi: [10.1086/308492](https://doi.org/10.1086/308492)
- Kowal, G., de Gouveia Dal Pino, E. M., & Lazarian, A. 2012, *Physical Review Letters*, 108, 241102, doi: [10.1103/PhysRevLett.108.241102](https://doi.org/10.1103/PhysRevLett.108.241102)
- Kowal, G., Falceta-Gonçalves, D. A., Lazarian, A., & Vishniac, E. T. 2017, *ApJ*, 838, 91, doi: [10.3847/1538-4357/aa6001](https://doi.org/10.3847/1538-4357/aa6001)
- Kowal, G., & Lazarian, A. 2010, *ApJ*, 720, 742, doi: [10.1088/0004-637X/720/1/742](https://doi.org/10.1088/0004-637X/720/1/742)
- Krumholz, M. R., Crocker, R. M., Xu, S., et al. 2020, *MNRAS*, 493, 2817, doi: [10.1093/mnras/staa493](https://doi.org/10.1093/mnras/staa493)
- Kulsrud, R., & Pearce, W. P. 1969, *ApJ*, 156, 445, doi: [10.1086/149981](https://doi.org/10.1086/149981)
- Lazarian, A. 2005, in *American Institute of Physics Conference Series*, Vol. 784, *Magnetic Fields in the Universe: From Laboratory and Stars to Primordial Structures.*, ed. E. M. de Gouveia dal Pino, G. Lugones, & A. Lazarian, 42–53, doi: [10.1063/1.2077170](https://doi.org/10.1063/1.2077170)
- Lazarian, A. 2006, *ApJL*, 645, L25, doi: [10.1086/505796](https://doi.org/10.1086/505796)
- . 2016, *ApJ*, 833, 131, doi: [10.3847/1538-4357/833/2/131](https://doi.org/10.3847/1538-4357/833/2/131)
- Lazarian, A., & Beresnyak, A. 2006, *MNRAS*, 373, 1195, doi: [10.1111/j.1365-2966.2006.11093.x](https://doi.org/10.1111/j.1365-2966.2006.11093.x)
- Lazarian, A., & Vishniac, E. T. 1999, *ApJ*, 517, 700, doi: [10.1086/307233](https://doi.org/10.1086/307233)
- Lazarian, A., Vishniac, E. T., & Cho, J. 2004, *ApJ*, 603, 180, doi: [10.1086/381383](https://doi.org/10.1086/381383)
- Lazarian, A., & Yan, H. 2014, *ApJ*, 784, 38, doi: [10.1088/0004-637X/784/1/38](https://doi.org/10.1088/0004-637X/784/1/38)
- Lemoine, M., & Malkov, M. A. 2020, *MNRAS*, 499, 4972, doi: [10.1093/mnras/staa3131](https://doi.org/10.1093/mnras/staa3131)
- Lithwick, Y., & Goldreich, P. 2001, *ApJ*, 562, 279, doi: [10.1086/323470](https://doi.org/10.1086/323470)
- López-Barquero, V., Farber, R., Xu, S., Desiati, P., & Lazarian, A. 2016, *ApJ*, 830, 19, doi: [10.3847/0004-637X/830/1/19](https://doi.org/10.3847/0004-637X/830/1/19)
- Luo, Q. Y., & Wu, D. J. 2010, *ApJL*, 714, L138, doi: [10.1088/2041-8205/714/1/L138](https://doi.org/10.1088/2041-8205/714/1/L138)

- Lynn, J. W., Parrish, I. J., Quataert, E., & Chandran, B. D. G. 2012, *ApJ*, 758, 78, doi: [10.1088/0004-637X/758/2/78](https://doi.org/10.1088/0004-637X/758/2/78)
- Maron, J., & Goldreich, P. 2001, *ApJ*, 554, 1175, doi: [10.1086/321413](https://doi.org/10.1086/321413)
- Matthaeus, W. H., Goldstein, M. L., & Roberts, D. A. 1990, *J. Geophys. Res.*, 95, 20673, doi: [10.1029/JA095iA12p20673](https://doi.org/10.1029/JA095iA12p20673)
- Nava, L., & Gabici, S. 2013, *MNRAS*, 429, 1643, doi: [10.1093/mnras/sts450](https://doi.org/10.1093/mnras/sts450)
- Noerdlinger, P. D. 1968, *PhRvL*, 20, 1513, doi: [10.1103/PhysRevLett.20.1513](https://doi.org/10.1103/PhysRevLett.20.1513)
- Orlando, E. 2018, *MNRAS*, 475, 2724, doi: [10.1093/mnras/stx3280](https://doi.org/10.1093/mnras/stx3280)
- Padovani, M., Ivlev, A. V., Galli, D., & Caselli, P. 2018, *A&A*, 614, A111, doi: [10.1051/0004-6361/201732202](https://doi.org/10.1051/0004-6361/201732202)
- Palmer, I. D. 1982, *Reviews of Geophysics and Space Physics*, 20, 335, doi: [10.1029/RG020i002p00335](https://doi.org/10.1029/RG020i002p00335)
- Parker, E. N. 1965, *Planet. Space Sci.*, 13, 9, doi: [10.1016/0032-0633\(65\)90131-5](https://doi.org/10.1016/0032-0633(65)90131-5)
- Post, R. F. 1958, *Proc. of Second U.N. Int. Conf. on Peaceful Uses of Atomic Energy*, Vol. 32, Paper A/Conf. 15/P/377, Geneva, pp. 245-265
- Ptuskin, V. S., Moskalenko, I. V., Jones, F. C., Strong, A. W., & Zirakashvili, V. N. 2006, *ApJ*, 642, 902, doi: [10.1086/501117](https://doi.org/10.1086/501117)
- Qin, G., Matthaeus, W. H., & Bieber, J. W. 2002, *ApJL*, 578, L117, doi: [10.1086/344687](https://doi.org/10.1086/344687)
- Richardson, L. F. 1926, *Proceedings of the Royal Society of London Series A*, 110, 709, doi: [10.1098/rspa.1926.0043](https://doi.org/10.1098/rspa.1926.0043)
- Schlickeiser, R. 2002, *Cosmic Ray Astrophysics*, ed. R. Schlickeiser
- Schlickeiser, R., Caglar, M., & Lazarian, A. 2016, *ApJ*, 824, 89, doi: [10.3847/0004-637X/824/2/89](https://doi.org/10.3847/0004-637X/824/2/89)
- Schlickeiser, R., & Miller, J. A. 1998, *ApJ*, 492, 352, doi: [10.1086/305023](https://doi.org/10.1086/305023)
- Schlickeiser, R., & Oppotsch, J. 2017, *ApJ*, 850, 160, doi: [10.3847/1538-4357/aa970e](https://doi.org/10.3847/1538-4357/aa970e)
- Singer, H. J., Heckman, G. R., & Hirman, J. W. 2001, *Washington DC American Geophysical Union Geophysical Monograph Series*, 125, 23, doi: [10.1029/GM125p0023](https://doi.org/10.1029/GM125p0023)
- Sioulas, N., Isliker, H., Vlahos, L., Koumtzis, A., & Pisokas, T. 2020, *MNRAS*, 491, 3860, doi: [10.1093/mnras/stz3259](https://doi.org/10.1093/mnras/stz3259)
- Voelk, H. J. 1975, *Reviews of Geophysics and Space Physics*, 13, 547, doi: [10.1029/RG013i004p00547](https://doi.org/10.1029/RG013i004p00547)
- Xu, S., & Lazarian, A. 2018, *ApJ*, 868, 36, doi: [10.3847/1538-4357/aae840](https://doi.org/10.3847/1538-4357/aae840)
- . 2020, *ApJ*, 894, 63, doi: [10.3847/1538-4357/ab8465](https://doi.org/10.3847/1538-4357/ab8465)
- Xu, S., Lazarian, A., & Yan, H. 2015, *ApJ*, 810, 44, doi: [10.1088/0004-637X/810/1/44](https://doi.org/10.1088/0004-637X/810/1/44)
- Xu, S., & Yan, H. 2013, *ApJ*, 779, 140, doi: [10.1088/0004-637X/779/2/140](https://doi.org/10.1088/0004-637X/779/2/140)
- Xu, S., Yan, H., & Lazarian, A. 2016, *ApJ*, 826, 166, doi: [10.3847/0004-637X/826/2/166](https://doi.org/10.3847/0004-637X/826/2/166)
- Yan, H., & Lazarian, A. 2002, *Physical Review Letters*, 89, B1102+, doi: [10.1103/PhysRevLett.89.281102](https://doi.org/10.1103/PhysRevLett.89.281102)
- . 2003, *ApJL*, 592, L33, doi: [10.1086/377487](https://doi.org/10.1086/377487)
- . 2004, *ApJ*, 614, 757, doi: [10.1086/423733](https://doi.org/10.1086/423733)
- . 2008, *ApJ*, 673, 942, doi: [10.1086/524771](https://doi.org/10.1086/524771)